An Investigation of the Influence of Shaft Misalignment on Bending Stresses of Helical Gears with Lead Crown

M.A. Hotait, D. Talbot and A. Kahraman

Management Summary

In this study, the combined influence of shaft misalignments and gear lead crown on load distribution and tooth bending stresses is investigated. Upon conclusion, the experimental results are correlated with predictions of a gear load distribution model, and recommendations are provided for optimal lead crown in a given misalignment condition.

Introduction

Gears are highly engineered machine elements that must be designed not only to meet the torque, speed, life and noise requirements under nominal conditions, but also to compensate for adverse effects due to manufacturing errors, variations and elastic deformations of the support structures. In addition to the elastic deformation of the support and structures, manufacturing errors in the gears, shafts and housing must also be considered in the design. Assuming that perfectly aligned shafts support a gear pair in which the shafts, bearings and the housing are all rigid might lead to severe wear and noise problems.

A reasonably accurate gear pair, with a limited amount of tooth surface manufacturing errors and operated under ideal (no error and no deflection) support conditions, can be expected to exhibit a good load distribution along its face width. If the shafts are mounted on bearings with position errors, or the shafts, bearings and housing deflect under load, then the rotational axes of the gears will no longer be parallel to each other. These conditions cause a mismatch of meshing teeth, resulting in a non-uniform load distribution along the face width, with perhaps very little or no load on one side and a larger edge load on the other. Such poor load distribution conditions might result in contact and tooth bending stresses at the overloaded side that are higher than the allowable (designed) limits, thus triggering premature bending or contact fatigue failures. Such poor load distribution also accelerates the rate of wear at the gear tooth surfaces.

One widely accepted, practical solution to edge loading due to misalignments caused by manufacturing errors and shaft/bearing deflections is to machine the gear tooth profiles so that additional material is removed from the edges to form a convex tooth surface in the face width (lead) direction, or lead crown. A gear pair having a certain amount of lead crown when there are no shaft misalignments would reduce the stresses near the edges of the tooth, while increasing the stresses at the tooth center. In case of a certain amount of shaft misalignment, the load distribution is modified so that the excessive edge loading due to shaft misalignments is prevented.

Predicting gear load distribution and its resultant stresses has been a major research topic. A number of theoretical and computational studies (Refs. 1–10) were carried out, considering both static and dynamic loading conditions. These studies mostly used finite element or boundary element models of varying complexity and size to predict load distribution and gear stresses at the tooth root region. Some of these models allowed misalignments to gears in a certain direction to predict the resultant changes in the load distributions (Refs. 11–15). For instance, the study by Wagaj and Kahraman (Ref. 15) has shown that the tooth profile and lead modifications influence the contact pattern, load distribution and contact stresses significantly, and that the amount and shape of the tooth modifications requirements vary with misalignments.

Most of the computational studies listed above focused on the modification of the tooth in the involute direction to reduce gear transmission error, a common gear noise excitation. Therefore, the primary effort in validation of these models was applied to their predictions of static transmission error; experimental studies by Kahraman and Blankenship (Ref. 16) provided such data for validations of these models. They also showed experimentally that gear involute contact ratio and profile modifications can be adjusted to minimize such excitations. The same experiments were also used to relate the dynamic stress factors to gear transmission error (Ref. 17). Other experimental studies, starting with Kubo (Ref. 18), provide experimental root stress data for spur gears under both static and dynamic conditions. Houser (Ref. 19) provided a comprehensive database of measured root strains for gears

having tooth spacing errors. Oswald and Townsend (Ref. 20) compared analytical and experimental data for dynamic tooth load and fillet stresses of spur gears. And more recently, Baud and Velex (Ref. 21) published static and dynamic helical gears strain data to validate the root stresses of a finite element model.

A review of previous work reveals that, while influence of the profile modifications is well-studied—especially for spur gears—the number of experimental studies on the influence of the lead crown on helical gear pairs subjected to misalignments is quite limited. There is very little experimental data available on the relationship between the gear lead crown and shaft misalignments. The models cited above lack any validation in terms of their predictions of root stresses under misaligned conditions. In many practical applications, the amount of lead crown is still determined based on the trial-and-error method or past field experiments. It has been reported that applying lead crown increases root stresses in the middle of the gears, while eliminating edge loading. Any excessive amount of lead crown employed to eliminate the negative effects of shaft misalignments has the potential to increase the stresses at the center of the teeth beyond the stress levels caused by edge loading. Therefore, the relationship between the lead crown and shaft misalignment under varying torque values must be investigated, both experimentally and theoretically.

Investigation of the impact of shaft misalignments on the root stresses of gears with or without lead crown is the main focus of this study. Its first objective is to develop an experimental test program that will yield a root strain database of tightly controlled experiments for helical gears with misalignments and lead crown, thus quantifying the relationship between shaft mounting errors and gear lead crown modifications in terms of gear bending stresses. Wide ranges of shaft misalignments and magnitudes of lead crown will be considered in these experiments, as well as a wide range of transmitted torque. An existing gear contact model will be used to simulate these test conditions in order to describe the behavior observed in the experiments. The accuracy of the root strain prediction of the contact model will then be assessed, and design guidelines on lead crowning of helical gears with misalignment will be provided.

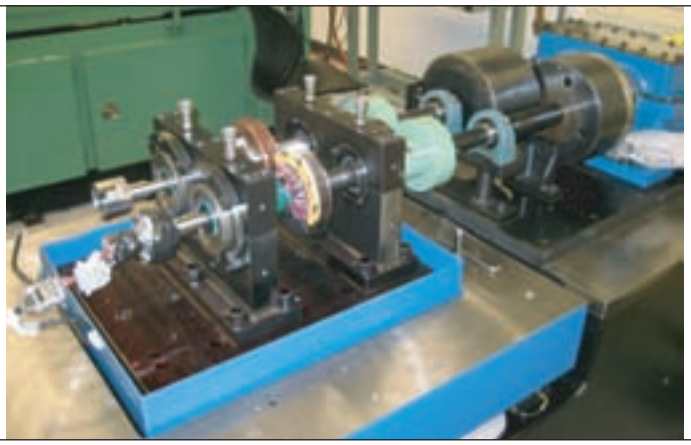

Figure 1—Gear test machine used in the study.

Table 1—Basic design parameters of the test gear pairs (all the dimensions are in mm unless specified).

Parameter	Drive Gear	Driven Gear
Number of Teeth	62	62
Normal Module	2.04	
Normal Pressure Angle (deg)	16	
Helix Angle (deg)	32.5	
Pitch Diameter	150.0	
Base Diameter	142.02	
Major Diameter	153.74	153.24
Minor Diameter	142.02	
Circular Tooth Thickness	2.46	
Lead Crown (λ)	Variable	
Involute Crown	0.012	0

Experimental Setup

A power circulatory-type gear dynamics test machine—shown in Figure 1—was used for the experiments. In this arrangement, the test gear pair and a reaction gear pair are connected by flexible shafts and elastomer couplings, ensuring full isolation of the reaction gear pair from the test side. The test pair—a driving gear and a driven gear—were mounted on parallel shafts, which are supported by a pair of spherical roller bearings. The bearings are housed by bearing caps that are held by rigid bearing pedestals. The bearing caps of varying eccentricity can be clocked in any direction to obtain shaft misalignments of various magnitudes in any desired direction. A split coupling is used to manually hang calibrated weights through a torque arm to achieve constant gear torque values up to 500 Nm, or a mesh force up to 6,600 N. Test gears and support bearings were jet-lubricated to minimize adverse frictional effects.

Four helical test gears (named *g*1, *g*2, *g*3, and *g*4) were used in these experiments. Table 1 lists basic design parameters of the test gears. Gear g1 of the right-hand is the strain-gauged driving gear, while left-handed gears *g*2, *g*3 and *g*4 form the driven gears. Driving gear *g*1 has a nominal tooth profile crown modification of 12 µm in the involute direction but has no lead modification. The driven gears have no

continued

Figure 2—Test gears used in this study.

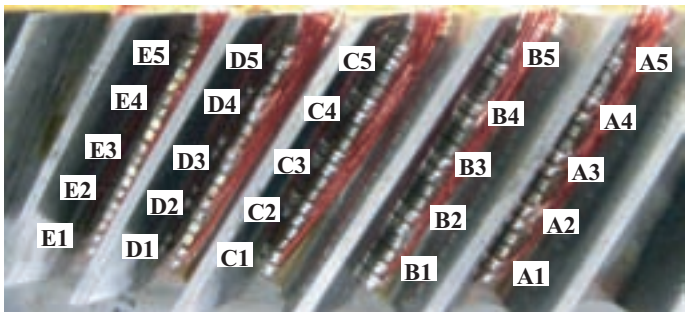

Figure 3—A view of the strain gauges on gear *g*1.

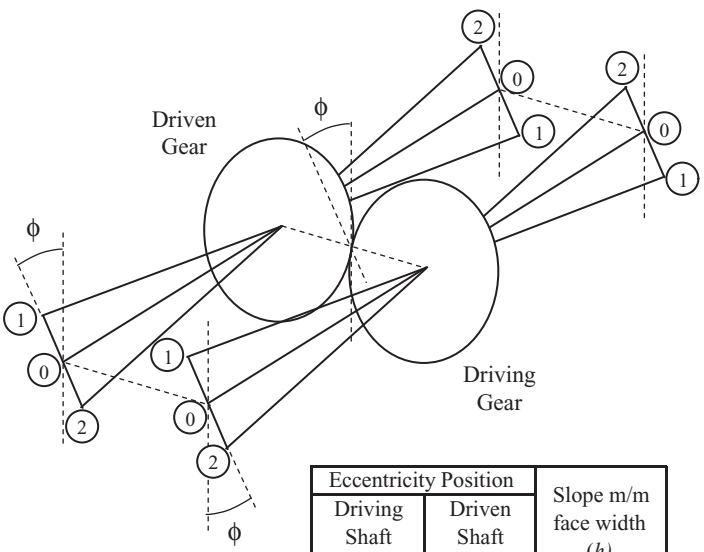

Eccentricity Position		Slope m/m face width (*h*)
Driving Shaft Bearing	Driven Shaft Bearing	
1	2	-0.002
0	2	-0.001
0	0	0
0	1	0.001
2	1	0.002

Figure 4—Definition of shaft misalignments.

modifications in the involute direction, yet they have varying amounts of circular lead crown λ ($\lambda = 0$) for gear *g*2, $\lambda = 12$ µm for gear *g*3 and $\lambda = 25$ µm for gear *g*4). These desired modification amounts were obtained by precise grinding of the gear profiles after case hardening. This way, gear pairs *g*1–*g*2, *g*1–*g*3 and *g*1–*g*4 have the same total involute crown value of 12 µm, and three levels of total lead crown ($\lambda = 0$, 12 and 25 µm). The test gears are shown in Figure 2.

Five consecutive teeth of gear g1 were strain-gauged as shown in Figure 3. At the root of each of these five teeth (A through E), five gauges were placed and equally spaced along the face width direction, bringing the total number of gauges to 25. Gauge strips (measurement group EA-06-031PJ-120) were used in order to ensure precise alignment of the gauges, slightly below the start of active profile, at a radius of 72.22 mm (roll angle). Only five of the gauges on each strip were activated, resulting in gauges at 2.7, 6.1, 9.6, 13.0 and 16.5 mm along the face width, measured from one edge.

With the concentric bearing caps (the outside diameter and the bore of the caps are concentric), the test gear shafts are positioned parallel to each other, without misalignments. That is because caps of a certain bore eccentricity forces the shafts to be misaligned at the bearing locations by the same amount, and thus a shaft misalignment is initiated. A set of bearing caps having an eccentricity of 125 µm is used for the misalignments. When two of these caps are used on a shaft with the eccentricities in opposite direction, a total misalignment of 250 µm is achieved over a span of 250 mm, resulting in a misalignment of $h = 0.001$ m/m. Pairing this shaft with one having no misalignment results in a total gear misalignment of $h = 0.001$ m/m. If this misaligned gear shaft is matched with another shaft having the same amount of misalignment in the opposite direction, the gear pair misalignment is doubled to $h = 0.002$ m/m. Figure 4 shows how the two levels of shaft misalignment in the direction of line of

action are obtained in both directions to achieve total slopes of $h = \pm 0.001$and $h = \pm 0.002$ m/m, in addition to the case of zero misalignment. For example, when the directions of eccentricities on the driving shaft are at position 1, and those on the driven shaft are at position 2 (as in Figure 4), one obtains h = –0.002 m/m face width. Position 2 on the driving shaft and position 1 on the driven shaft, meanwhile, represent a misalignment of $h = 0.002$ m/m. Table 2 shows the test matrix considered in this study. Gear pairs $g1$–$g2$, $g1$–$g3$ and $g1$–$g4$ were tested under the five shaft misalignment values of $h = 0, \pm 0.001$ and ± 0.002 m/m, resulting in a total of 15 tests. Each of these tests was performed at discrete torque values of 100, 200, 300, 400 and 500 Nm, bringing the total number of tests to 75.

All of the tests were performed at a constant rotational speed of 200 rpm in order to avoid any dynamic effects. Gauges on tooth C (C1 through C5) were considered as the primary gauges, and data from these five gauges were collected and analyzed simultaneously to capture the variation of root strains along the facewidth. Additional tests were also performed with active gauges of A3, B3, C3, D3 and E3 to ensure that the tooth-to-tooth variability of the measured strain signals is minimal. The strain signals were taken out of the shaft through a slip ring, put through a multi-channel strain-gauge conditioning unit (Vishay 2300), acquired by a NI PXI–4472 dynamic signal acquisition module integrated into the multi-purpose NI PXI–1042, and finally processed using a *LabView* program.

Experimental Results

The experimental data for the case of no misalignment and no lead crown will be presented as the baseline condition. As such, gear pair $g1$–$g2$ is used with no shaft misalignments; i.e., $\lambda = 0$ and $h = 0$. Figure 5 shows the strain-time histories of the gauges of tooth C gauges throughout one loading cycle—at four discrete torque levels of 100, 200, 300 and 400 Nm. Several observations can be made from Figure 5; first, each gauge exhibits only tensile strains, indicating that efforts to move the gauges to a location as close to SAP as possible was successful. Gauges C1 and C5 measure slightly less load than gauges at the middle section of the tooth, with C3 having the highest strains. Each gauge is loaded for slightly longer than two complete mesh cycles. That is in line with the value of the theoretical total contact ratio of the gear pair. The measured strain signal for gauge C1 leads the other gauges since that side of the contact is initiated at that side of gear $g1$. The root strains measured along the face width indicate that the load distribution is quite uniform. Moreover, the increase in strain levels is almost linear with torque transmitted,

continued

Table 2. Test matrix considered in this study.

Gear Pair	Total Lead Crown λ(μm)	Misalignment *h* (m/m)	Torque *T*(Nm)
1	0	0 +0.001 –0/001 +0.002 –0.002	100–500
2	12.5	0 +0.001 –0/001 +0.002 –0.002	100–500
3	25	0 +0.001 –0/001 +0.002 –0.002	100–500

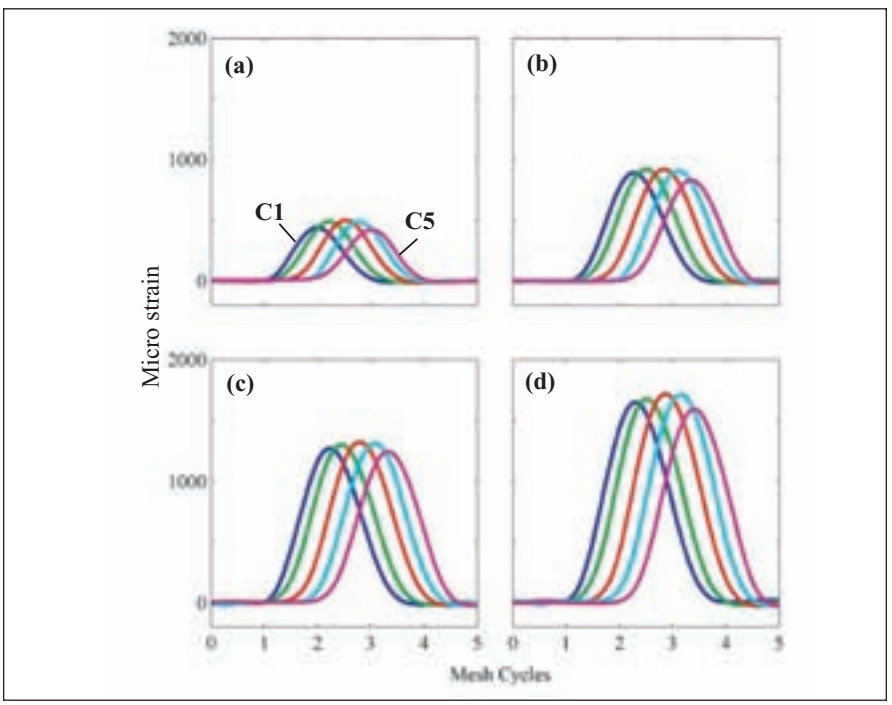

Figure 5—Measured strain time histories for gear pair $g1$–$g2$ having $\lambda = 0$ at $h = 0$—(a) $T = 100$ Nm; (b) $T = 200$ Nm; (c) $T = 300$ Nm; and (d) $T = 400$ Nm.

indicating that gear tooth deformations are linearly proportional to the gear mesh force.

Next, four different misalignments of $h = \pm 0.001$ m/m and ± 0.002 m/m are applied to the same gear pair $g1$–$g2$ at $T = 200$ Nm, and the resultant changes in root strains were compared to the baseline case of $h = 0$. Figure 6 shows the measured strain signals from gauges of tooth C for different h. A dramatic change in the root strains is observed with h. When $h < 0$, load is shifted to the edge near C1, resulting in significantly larger strains measured by this gauge in Figure 6 (a) and (b), while gauge C5 is very lightly loaded. The opposite is true for $h > 0$, where C5 bears the maximum strain while C1 records the lowest strain values. Both Figure 6 (a), for $h = -0.002$ m/m, and Figure 6 (e), for $h = 0.002$ m/m, represent severe edge-loading conditions that must be eliminated through lead crown. In these extreme cases, the measured maximum strains were about 45–60% higher than the maximum strain value measured by gauge C3 in Fig. 6 (c) for h = 0.

Figure 7 shows the measured strain data from gear pair $g1$–$g3$ at the same load and misalignment levels as in Figure 6; this gear pair has a total lead crown of $\lambda = 12$ µm. As a result, Figure 7 (c), for $h = 0$, indicates that the strains at the edges are reduced somewhat, while gauge C3 measures more strain than that of Figure 6 (c). This allows compensation of edge loading in Figure 7(e) for $h = 0.002$ m/m, while the load sharing in Figure 7(a) and (b) for $h < 0$ is still rather poor. Similarly, Figure 8 shows the same data, but now for gear pair $g1$–$g4$, which has a total lead crown of $\lambda =$ µm. In this figure, no sign of edge loading is evident, even for extremes of h. In Figure 8 (a), for $h = -0.002$ m/m, the maximum strain is at gauge C2, while it is gauge C4 for $h = 0.002$ m/m in Figure 8 (e). Both suggest that the amount of λ was sufficiently large for this gear pair under such misalignment conditions to prevent edge loading. The same behavior observed in Figures 6–8 for $T = 200$ Nm was seen in other tested torque levels as well.

Figure 9 provides a direct comparison of the variation of maximum root strains along the gear face width between λ and h. In Figure 9 (a), for gear pair g1–g2 ($\lambda = 0$), the slope of the measured maximum strains is positive for $h > 0$ and negative for $h < 0$. Given this data, one would reasonably expect the curves for various h values to intersect on the mid-plane of the gears—at 10 mm from the tooth edge—while in fact they cross at about 8 mm from the edge. This is perhaps due to unavoidable shaft misalignments within the test machine tolerances. In Fig. 9 (a), an allowable misalignment tolerance band of $h = \in [-0.002, 0.002]$ results in nearly 50% more strain near the edges. Considering that gauges C1 and C5 were two to three mm away from the tooth edges, the strain values at the edges should be even higher. In fact, the maximum strain distributions in Figure 9 (b), for gear pair $g1$–$g4$ with $\lambda = 25$ µm, introduce a convex-shaped distribution of the maximum root strain along the face width.

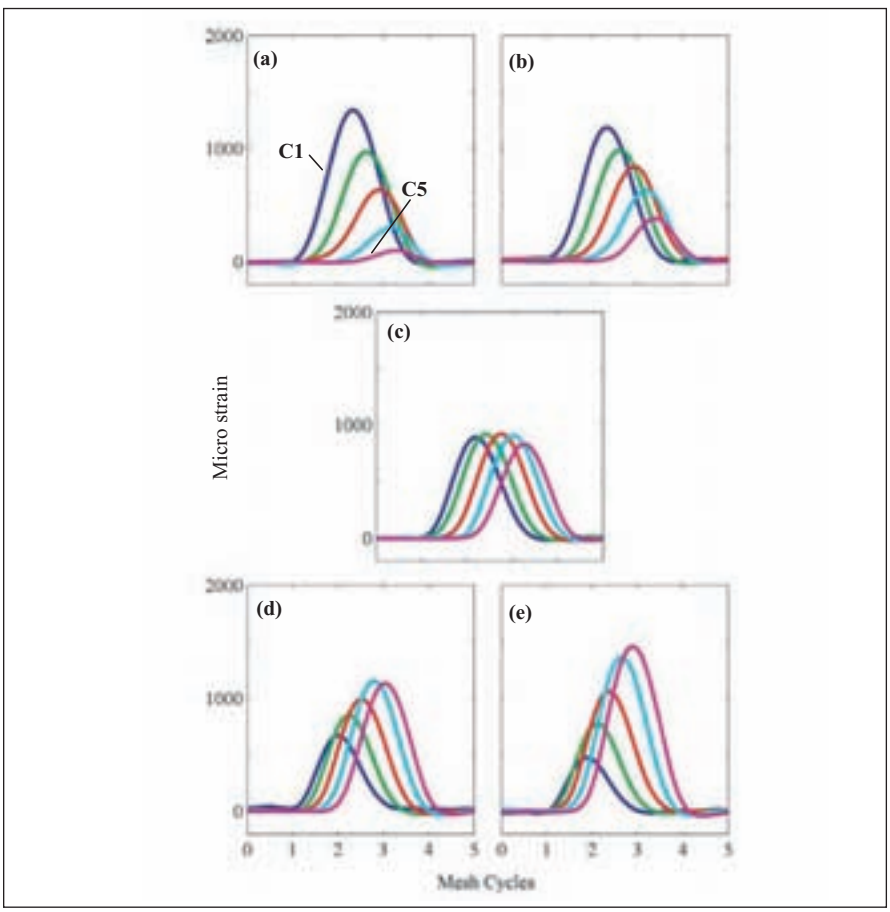

Figure 6—Measured strain time histories for gear pair $g1$–$g2$ having $\lambda = 0$ at $T = 200$ Nm—(a) $h = -0.002$ m/m; (b) $h = -0.001$ m/m; (c) $h = 0$; (d) $h = 0.001$ m/m; and (e) $h = 0.002$ m/m.

Comparison to Predictions

In this section, an existing gear contact model will be used to describe the trends exhibited by the experimental data. The model first computes the load distribution by using an existing load distribution model called LDP (Ref. 22), and then employs a three-dimensional finite element model to predict the root strains resulting from the computed load distribution (Ref. 22). LDP makes its prediction by first predicting the contact zone between the mating parts; next, for each point along this zone, the elastic deformation of each part is computed in the form of a compliance matrix. The elastic deformations considered include bending and shear deflections, base rotation and translation, as well as the local contact deflections of the teeth. Continuity and equilibrium conditions are then enforced. The continuity conditions assume initial separations and introduce a slack variable that tracks whether a given point is in contact or not. The initial separations

considered in this study include micro-geometry modification of both parts and misalignment. The load distribution is then calculated from these conditions for each time-step through a rotation of one base pitch and using a modified, Simplex-type algorithm (Ref. 22). The load distribution predicted in LDP is then used as the impetus for the finite element model to calculate the predicted root stress. The 3D finite element model (Ref. 23) employs 20-noded isoparametric elements in order to capture bending and shear effects. Because the contact zone and the load distribution are previously calculated, the stiffness matrix only needs to be factored once, and different nodal solutions for individual time-step loading case can be calculated simultaneously. This is advantageous because factoring the stiffness matrix is the most time-consuming step. After applying the load distribution and obtaining the nodal solutions, principal stress solutions are obtained for the full model and, most importantly, for the root.

The model employs user-defined radial and face width positions to interpolate strains from the finite element shape functions.

Figure 10 shows the predicted strain data for gear pairs $g1$–$g2$ (λ = 0) and $g1$–$g4$ (λ = 25 µm) at T = 200 Nm. Figures 10 (a), 10 (b) and 10 (c) refer to misalignment values of h = – 0.002, 0 and 0.002 m/m face width, respectively. These predictions are in qualitative agreement with the experimental strain-time histories presented earlier in Figures 6 and 8. The results for λ = 0 show discrepancies with the experimental results, primarily in the edge gauges; this is caused by the prediction of edge loading. Also, the incongruities observed in these predictions are primarily due to edge loading. Predictions for λ = 25 µm, on the other hand, exhibit a better correlation with the experimental results and show no incongruities resulting from the removal of predicted edge loading due to lead crown.

Figures 11 and 12 show the predicted maximum contact stress and maximum normal root stress distributions (on gear $g1$) for (λ = 0 and 25 µm) at T = 200 Nm. In both figures, the plots for λ = 0 demonstrate excessive edge loading and corner contact effects for h = – 0.002 and 0.002 m/m, which are eliminated in gear pair $g1$–$g4$ case, due to the addition of lead crown. The contact stress and root stress follow a similar trend as both are similarly affected by the same predicted load distribution.

Finally, Figure 13 compares the experimental maximum root strain curves of Figure 9 with the predicted values from Figure 12 at the locations of gauges specified earlier. In these figures the predicted and measured maximum strain measurements for λ = 0 and 25 µm are compared for h = –0.002, 0 and 0.002 m/m face width, individually. Here, regardless of the value of h, the maximum strain is measured by one of the gauges in the middle, suggesting that edge loading is eliminated. It is also noted that the maximum strains of a gear pair having λ = 25 µm for h = –0.002 and 0.002 m/m are comparable to the maximum strain value found in the gear pair having no lead crown. The difference is the location where this maximum strain is measured; under no-misalignment conditions, the maximum strain of the gear pair having λ = 25 µm is nearly 40% higher than that of the gear pair having no lead crown. This clearly demonstrates that, while eliminating adverse edge-loading effects, lead crown increases the bending stresses rather significantly. Therefore, any design that uses lead crown to accommodate shaft misalignments must also account for this increase in the root stresses. It is also noted in Figure 13 that the model predictions are in reasonably good agreement with the measured values. This model can therefore be used with confidence in determining the optimum amount of lead crown required to compensate for a given misalignment condition.

continued

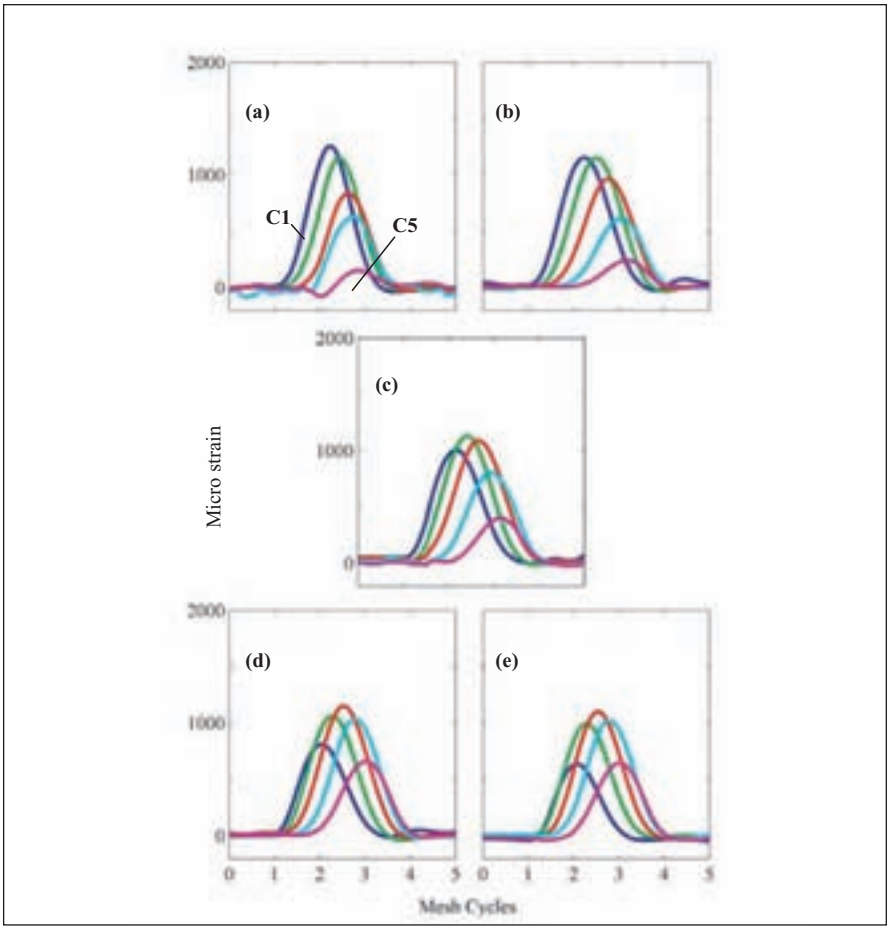

Figure 7—Measured strain time histories for gear pair $g1$–$g3$ having λ = 12 at T = 200 Nm; (a) h = –0.002 m/m; (b) h = –0.001 m/m; (c) h = 0; (d) h = 0.001 m/m; and (e) h = 0.002 m/m.

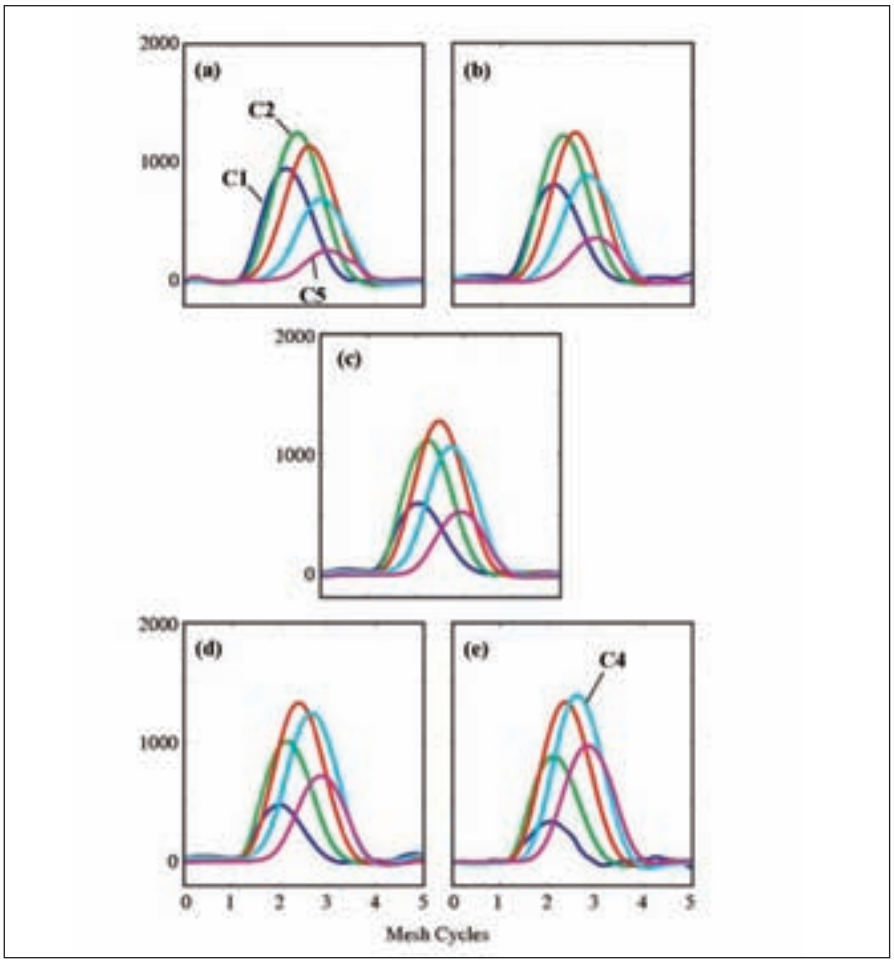

Figure 8—Measured strain-time histories for gear pair *g*1–*g*4 having λ = 25 at *T* = 200 Nm—(a) *h* = –0.002 m/m; (b) *h* = –0.002 m/m; (c) *h* = 0; (d) *h* = 0.001 m/m; and (e) *h* = 0.002 m/m.

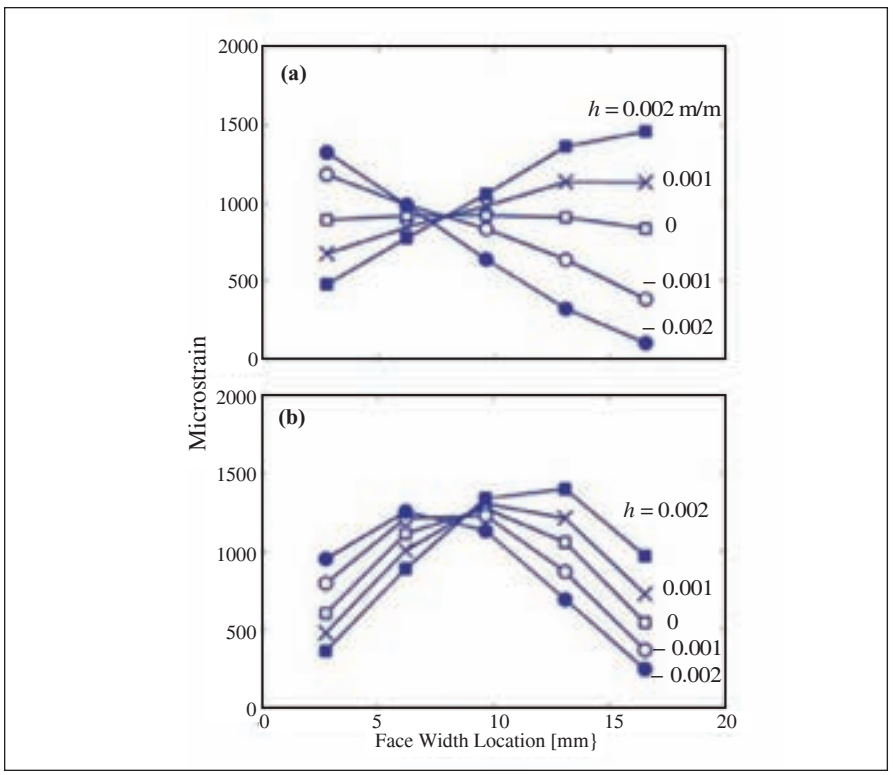

Figure 9—Variation of maximum root strain along the face width with *h* at *T* = 200 Nm for (a) λ = 0 and (b) λ = 25 μm.

Conclusions

The combined influence of shaft misalignments and gear lead crown on the load distribution and tooth bending stresses was investigated experimentally. An experimental study was performed by using a set of helical gear pairs having various amounts of lead crown. Gears were operated under tightly controlled shaft misalignments introduced in the direction of the line of action; the distribution of the root stresses was measured for various lead crown values. The experimental results were then compared to the predictions of a gear load distribution model to demonstrate good correlation. It was also shown that the amount of lead crown must be defined as a function of expected gear misalignment conditions. While edge loading was eliminated, excessive lead crown values were shown to increase maximum root and contact stresses.

Acknowledgment

The authors thank General Motors Powertrain for supporting an earlier study on this topic, and Mr. Dan Coffey for his expertise in the design and instrumentation of gears.

References

1. Chen, Y. C., and C.B. Tsay. "Stress Analysis of Helical Gear Set with Localized Bearing Contact," *Finite Elements in Analysis and Design*, 2002, 38, pp. 707–723.

2. Guibault, R., C. Gosselin and L. Cloutier. "Express Model for Load Sharing and Stress Analysis in Helical Gears," J*ournal of Mechanical Design*, 2005, 127(6), pp. 1161–1172.

3. Litvin, F. L., J.S. Chen, J. Lu and R.F. Handschuh. "Application of Finite Element Analysis for Determination of Load Share, Real Contact Ratio, Precision of Motion and Stress Analysis," *Journal of Mechanical Design*, 1996, 118 (4), pp. 561–566.

4. Clapper, M. L., and D. Houser. "A Boundary Element Procedure for Predicting Helical Gear Root Stresses and Load Distribution Factors," 94FTM6 American Gear Manufacturers Association, 1994, ISBN: 1–55589–640–5.

5. Gagnon, P., C. Gosselin and L. Cloutier.

"Analysis of Spur, Helical, and Straight Bevel Gear Teeth Deflection by Finite Strip Method," *Journal of Mechanical Design*, 1996, 119 (4), pp. 421–426

6. Guingand, M., J.P. Vaujany and Y. Icard. "Fast Three-Dimensional Model Quasi-Static Analysis of Helical Gears Using the Finite Prism Method," *Journal of Mechanical Design*, 2004, 126 (6), pp. 1082–1088.

7. Vijayakar, S. M. "Finite Element Methods for Quasi-Prismatic Bodies with Application to Gears," Ph.D. Dissertation, 1987, The Ohio State University.

8. Richard, E. D., R. Echempati and J. Ellis. "Design and Stress Analysis of Gears Using the Boundary Element Method," DETC98/PTG-5791, 1998 ASME DETC Power Transmission and Gearing Conference, Atlanta, USA.

9. Sfakiotakis, V. G., J.P. Vaitsis and N.K. Anifantis. "Numerical Simulation of Conjugate Spur Gear Action," *Computers and Structures*, 2001, 79 (12), pp. 1153–1160.

10. Coy, J. J., and C.H. Choa. "A Method of Selecting Grid Size to Account for Hertz Deformation in Finite Element Analysis of Spur Gears," *ASME Journal of Mechanical Design*, 1091, 103, pp. 759–766.

11. Guibault, R., C. Gosselin and L. Cloutier. "Helical Gears, Effect of Tooth Deviations and Tooth Modifications on Load Sharing and Fillet Stresses," *ASME Journal of Mechanical Design*, 2006, 128 (2), pp. 444–456.

12. Haigh, J., and J.N. Fawcett. "Effects of Misalignment on Load Distribution in Large Facewidth Helical Gears," *Journal of Multi-Body Dynamics, Proceedings of Institution of Mechanical Engineers*, 2003, 217(2), pp. 93–98.

13. Kawalec, A., J. Wiktor and D. Ceglarek. "Comparative Analysis of Tooth-Root Strength Using ISO and AGMA Standards in Spur and Helical Gears with FEM-based Verification," *Journal of Mechanical Design*, 2006, 128, pp. 1141–1158.

14. Lee, C., H.H. Lin, F.B. Oswald and D.P. Townsend. "Influence of Linear Profile Modification and Loading Conditions on the Dynamic Tooth Load and Stress of High-Contact-Ratio Spur Gears," *Journal of Mechanical Design*, 1991, 113, pp. 473–480.

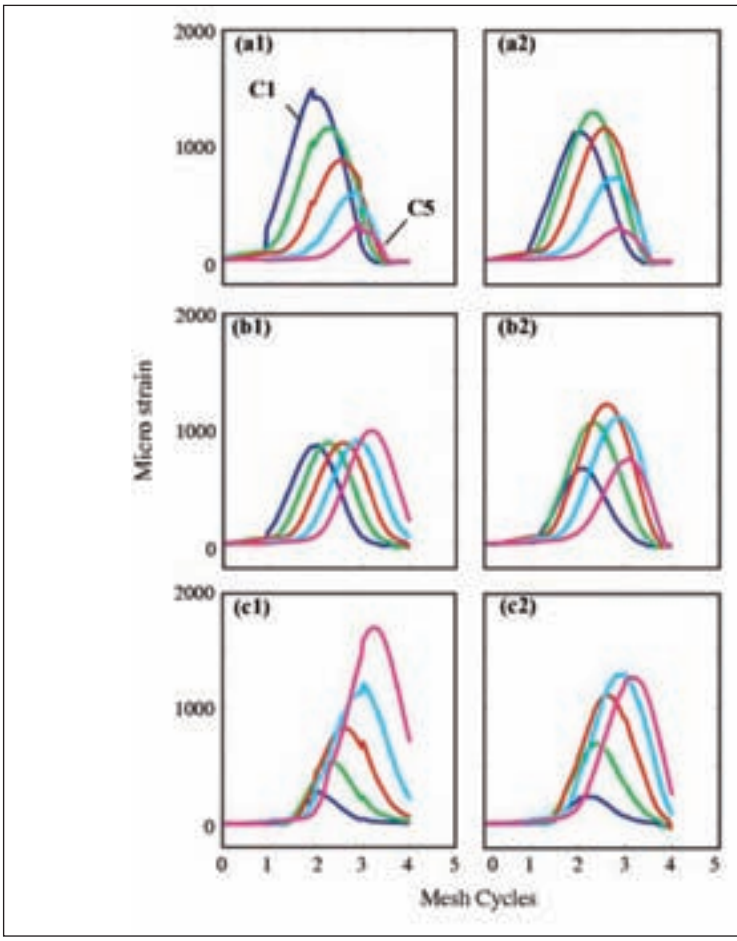

Figure 10—Predicted strain-time histories at *T* = 200 Nm—(a1) *h* = –0.002 m/m and λ = 0; (a2) *h* = –0.002 m/m, λ = 25 µm; (b1) *h* = 0 and λ = 0; (b2) *h* = 0 and λ = µm; (c1) *h* = 0.002 m/m and λ = 0; and (c2) *h* = 0/002 m/m and λ = 25 µm.

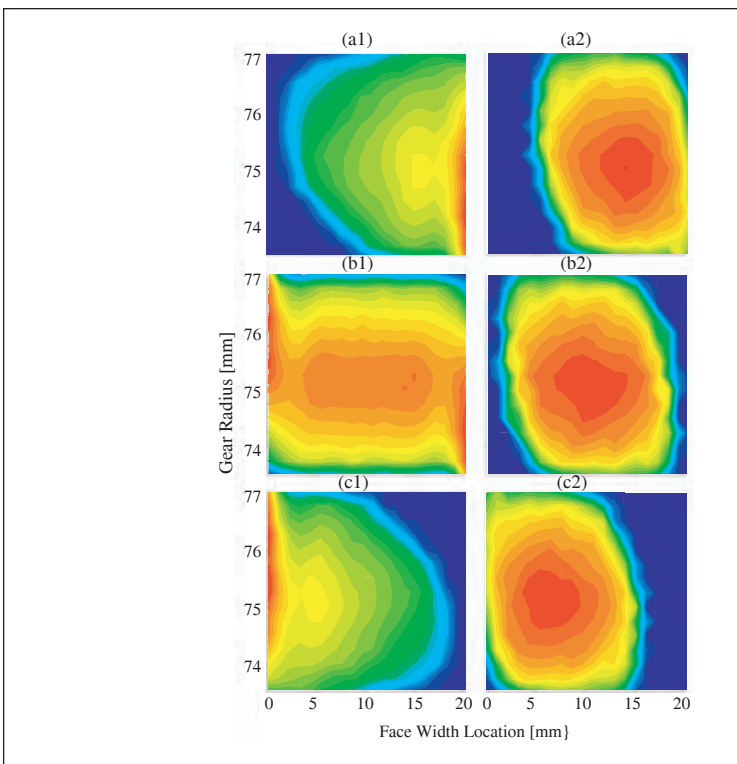

Figure 11—Predicted maximum contact stress distribution at *T* = 200 Nm—(a1) *h* = –0.002 m/m and λ = 0; (a2) 0.002 *h* = –0.002 m/m and λ = 25 µm; (b1) *h*= 0 and λ = 0; (b2) *h* = 0 and λ = 25 µm; (c1) *h* = 0.002 m/m and λ = 0; and (c2) *h* = 0.002 m/m and λ = 25 µm.

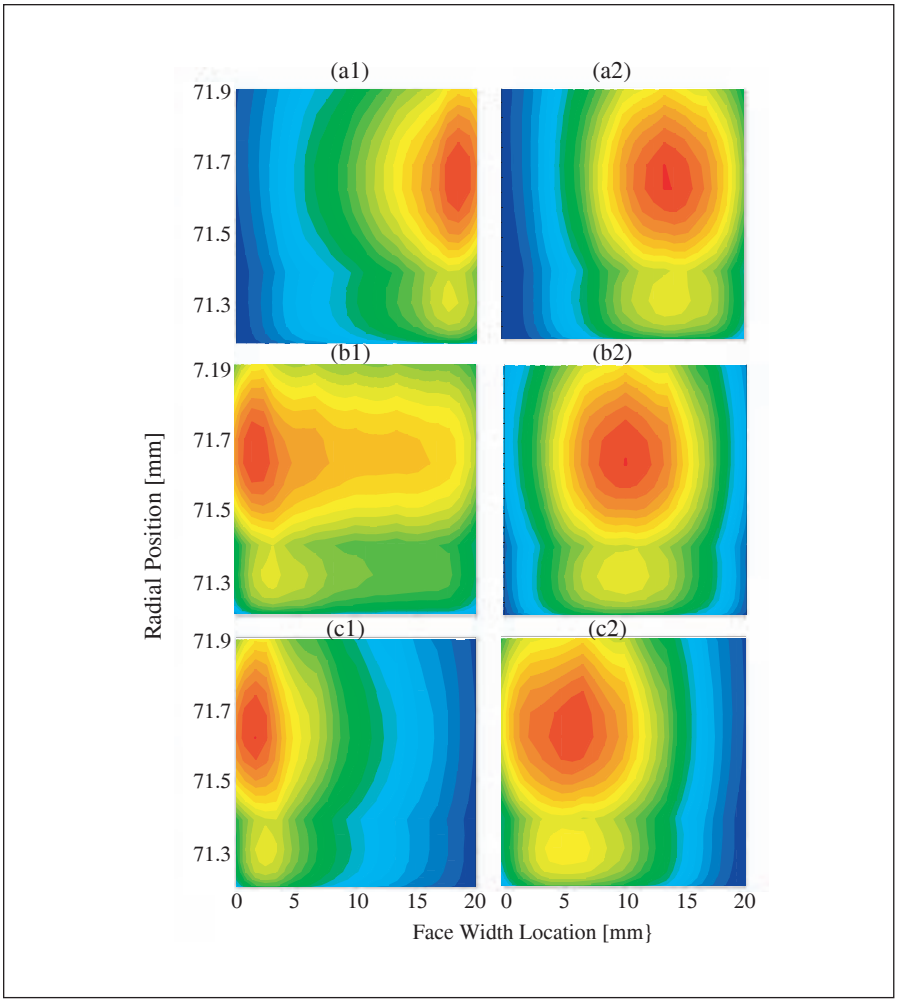

Figure 12—Predicted maximum root stress distribution at T = 200 Nm—(a1) h = –0.002 and λ = 0; (a2) h = –0.002 m/m and λ = 25 µm; (b1) h = 0 and λ = 0; (b2) h = 0 and λ = 25 µm; (c1) h = 0.002 m/m and λ = 0; and (c2) h = 0.002 m/m and λ = 25 µm.

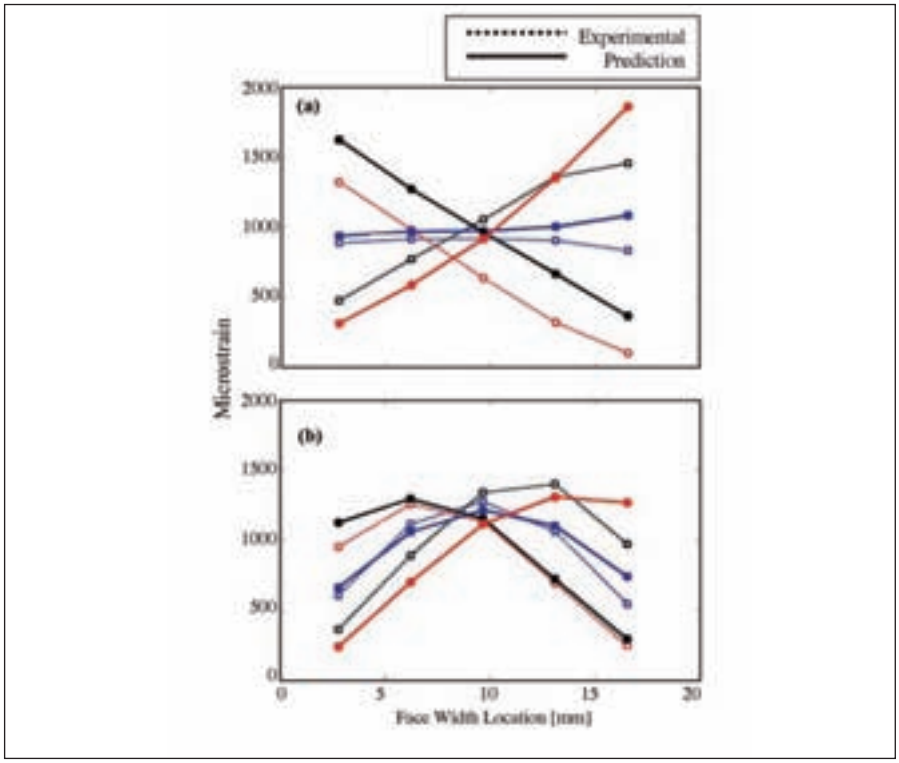

Figure 13—Comparison of measured and predicted maximum root strain along the face width at T = 200 Nm—(a) λ = 0 and (b) λ = 25 µm.

15. Wagaj, P. and A. Kahraman. "Influence of Tooth Profile Modification on Helical Gear Durability," *Journal of Mechanical Design*, 2002, 124(3), pp. 501–510.

16. Kahraman, A. and G.W. Blankenship. "Effect of Involute Tip Relief on Dynamic Response of Spur Gear Pairs," *ASME Journal of Mechanical Design*, 1999, 121, pp. 313–315.

17. Tamminana, V. K., A. Kahraman and S. Vijayakar. "A Study of the Relationship between the Dynamic Factors and the Dynamic Transmission Error of Spur Gear Pairs," *ASME Journal of Mechanical Design*, 2007, 129 (1), pp. 75–84.

18. Kubo, A. "Stress Condition, Vibrational Exciting Force and Contact Pattern of Helical Gears with Manufacturing Errors," *Journal of Mechanical Design*, 1978, 100, pp. 77–85.

19. Houser, D. R. "Analysis of the Influence of Errors and Stiffness on Dynamic Loads Developed in Spur and Helical Gears," Ph.D. Dissertation, 1969, University of Wisconsin.

20. Oswald, F. B. and D.P. Townsend. "Influence of Tooth Profile Modification on Spur Gear Dynamic Tooth Strain," 1995, NASA Technical Memorandum 106952.

21. Baud, S. and P. Velex. "Static and Dynamic Tooth Loading in Spur and Helical Geared Systems: Experiments and Model Validation," *ASME Journal of Mechanical Design*, 2002, 124 (2), pp. 334–346.

22. *Load Distribution Program* (Windows LDP), 2006, The Ohio State University.

23. Talbot, D. "Thin-Rim Gear Analysis Using Finite Elements," M.S. Thesis, 2007, The Ohio State University, Columbus, Ohio.

Mohammad Hotait and David Talbot *are both graduate research associates and Ph.D. candidates at the Mechanical Engineering Department of The Ohio State University.*

Ahmet Kahraman *is a professor of mechanical engineering at The Ohio State University, where he serves as the director of the Gear and Power Transmission Research Laboratory. His research focuses on several areas of power transmission and gearing, including gear system design and analysis; gear and transmission dynamics; gear lubrication and efficiency; wear and fatigue life prediction; and test methodologies. He is a fellow of ASME and member of SAE and STLE.*